Towards an Improvement in Aneurysm Assessment: Coupling 3D Reconstruction Tools with Engineering Know-How

Barry J. Doyle and Timothy M. McGloughlin

Centre for Applied Biomedical Engineering Research (CABER), Department of Mechanical and Aeronautical Engineering, and the Materials and Surface Science Institute, University of Limerick, Ireland.

ABSTRACT

Purpose: Currently, abdominal aortic aneurysms (AAAs), which are a permanent dilation of the aorta, are treated surgically when the maximum transverse diameter surpasses 5.0cm. AAA rupture occurs when the locally acting wall stress exceeds the locally acting wall strength. There is a need to review the current diameter-based criterion, and so it may be clinically useful to develop an additional tool to aid the surgical decision-making process. A Finite Element Analysis Rupture Index (FEARI) was developed. 3D reconstructions were also performed to aid endovascular aneurysm repair (EVAR).

Methods: Patient-specific AAAs were reconstructed using Mimics v12 and analysed for use with the FEARI. Previous experimental work on determination of ultimate tensile strengths (UTS) from AAA tissue samples was implemented in this study. By combining peak wall stress along with average regional UTS, a new approach to the estimation of patient-specific rupture risk has been developed. A further 4 AAA cases were reconstructed and analysed in Mimics v12 to determine stent-graft sizes and plan EVAR.

Results: A detailed examination of these cases utilising the FEARI analysis suggested that there was a possibility that some of the AAAs may have been less prone to rupture than previously considered. 3D reconstructions as a surgical guidance tool proved to be very effective in accurate device sizing and pre-surgical planning.

Conclusions: It is proposed that FEARI, used alongside other rupture risk factors, may improve the current surgical decision-making process. The use of FEARI as an additional tool for rupture prediction may provide a useful adjunct to the diameter-based approach in surgical decision-making. 3D reconstructions aid surgeons in planning EVAR, in particular in the case of extreme cases of aneurismal disease.

Keywords: Aneurysm, 3D reconstruction, Rupture, Prediction, Stress, Strength, Surgical Guidance.

INTRODUCTION

Cardiovascular disease is the leading cause of morbidity and premature death of modern era medicine. It is estimated that approximately 81 million people in the United States (US) currently have one or more of the many forms of cardiovascular disease, resulting in 1 in every 2.8 deaths, or approximately 900,000 deaths per year. Aneurysms form a significant portion of these cardiovascular related deaths and are defined as a permanent and irreversible localised dilation of a blood vessel greater than 50% of its normal diameter.[1] There is currently much debate as to the most appropriate time to surgically intervene and repair an abdominal aortic aneurysm (AAA),[2-8] with surgery often performed when the detected AAA exceeds 5.0-5.5cm in maximum diameter. AAA size will always be a concern of the clinician, however, previous research[9,10] has shown how AAAs smaller than 5.0cm in maximum diameter can also rupture. The reliability of the maximum diameter as the main criterion for rupture has been questioned recently, and a need for a more reliable clinical predictor of AAA rupture has been identified.[2-8,10-15] It is known that AAA rupture occurs when the locally acting wall stress exceeds the locally acting wall strength. Therefore, the AAA tissue strength must play an equal role to AAA wall stress in determining failure. A region of AAA wall that is under elevated wall stress may also have high wall strength, thus equalising its rupture potential. A novel rupture index was utilised as part of this study called the Finite Element Analysis Rupture Index (FEARI).[15] This index aides the surgical decision-making process by expressing the rupture potential of an aneurysm in terms of a numerical value. FEARI close to 1 indicates a high rupture potential, with values close to 0 expressing low propensity to rupture. Once the surgical intervention is decided, endovascular aneurysm repair (EVAR) is often the preferred choice. This minimally invasive technique has many benefits over traditional open repair.[16] Correct sizing of the medical device is paramount to the effectiveness of the device, as post-operative complications can arise.[16] This paper aims to examine the effectiveness of FEARI and also show how 3D reconstructions can be a useful surgical guidance tool.

METHODS

3D Reconstructions for FEARI

Spiral computed tomography (CT) data was used to reconstruct the infrarenal section of the aorta. As CT scanning is routinely performed on AAA patients scheduled for

repair, collection of this information involved no extra participation by the study subjects. CT scan data was obtained for 10 patients (male, n=6; female, n=4). These patient scans were obtained from the Midwestern Regional Hospital, Limerick, Ireland, and the University of Pittsburgh Medical Centre, Pittsburgh, PA, USA. All ten patients were either awaiting or had received AAA repair at the time of CT scan, as AAA diameters had reached or exceeded the current 5.0cm threshold for repair. CT scans were acquired using both the Somatom Plus 4 (Siemens AG, D-91052 Erlangen, Germany) and LightSpeed Plus (GE Medical Systems, General Electric Company) range of imaging equipment. All scans were single CT slices with a standard width x height of 512 x 512 pixels. Mean pixel size of scans was 0.742 ± 0.072 mm. The bodily structures of each subject were made visible using the non-ionic contrast dye, Optiray® (Mallinckrodt Inc., Convidien, MO, USA). 3D reconstructions were performed using the commercial software Mimics v12 (Materialise, Belgium). This reconstruction technique was validated with previous work performed by our group.[17,18] Briefly, a thresholding technique is applied to each scan in the series. This process assigns a pixel intensity value measured in Hounsfield units (HU) to each pixel in the image. From this, the HU value can be controlled so that only the regions of interest are thresholded. Following this technique, segmentation of the image is possible. This assigns a certain colour to a certain region of interest, in this case the diseased aorta. By applying this algorithm to the series of CT scans, a complete 3D reconstruction can be generated. This process can be seen in Figure 1. Assigning regions into different layers allows certain areas to be highlighted or removed depending on the desired region of interest. An example of this layered approach to reconstruction can be seen in Figure 2. In this particular reconstruction, all major internal structures were generated for illustration purposes. The iliac arteries were omitted from the FEARI reconstructions as they have been shown not to significantly alter the resulting wall stress distributions.[7] Patient-specific wall thickness was obtained using the equation proposed by Li and Kleinstreuer[19] shown in Eqn. 1, where t is wall thickness and Dia_{max} is the maximum diameter. The ILT was also included in the reconstructions as this structure has been shown to reduce wall stress.[11] The models developed by this method formed the basis for the finite element method (FEM) stress analysis. The pre-operative details of the ten cases examined can be seen in Table 1.

$$t = 3.9\left(\frac{Dia_{max}}{2}\right)^{-0.2892} \qquad \text{Eqn.1}$$

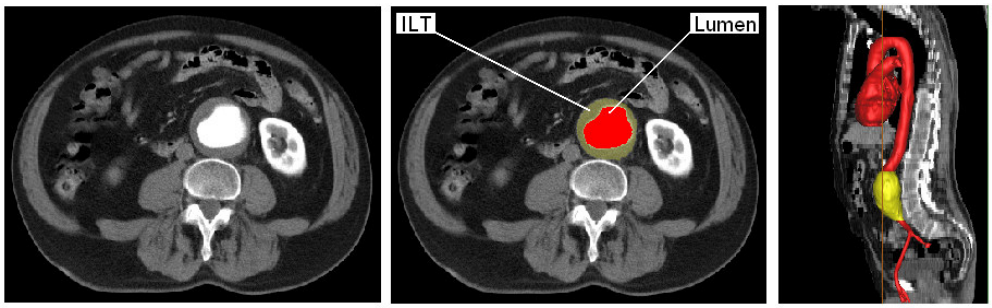

Figure 1: (A) Typical CT scan showing aneurysmal aorta in centre of image, (B) algorithm defines regions of interest and (C) software generates 3D reconstruction of desired regions.

Table 1: Pre-operative patient details for each study subject. Note that Ø is diameter.

Patient	*Sex*	*Max Ø (cm)*	*Wall Thickness (mm)*	*AAA Length (cm)*	*AAA Volume (cm^3)*	*ILT Volume (cm^3)*
1	Male	5.1	1.53	13.2	176.7	54.1
2	Male	5.8	1.48	11.2	192.4	122.8
3	Male	5.9	1.47	11.6	194.9	96.8
4	Female	5	1.54	9.3	136.9	38.4
5	Male	5.9	1.47	12.8	220.9	116.8
6	Male	7.4	1.37	14.3	311.6	147.6
7	Female	5.3	1.51	10.5	137.9	82.5
8	Female	6.2	1.48	9.7	61.6	29.1
9	Female	6.5	1.43	10.5	217.3	150.2
10	Male	9	1.29	11.7	445.5	124.5

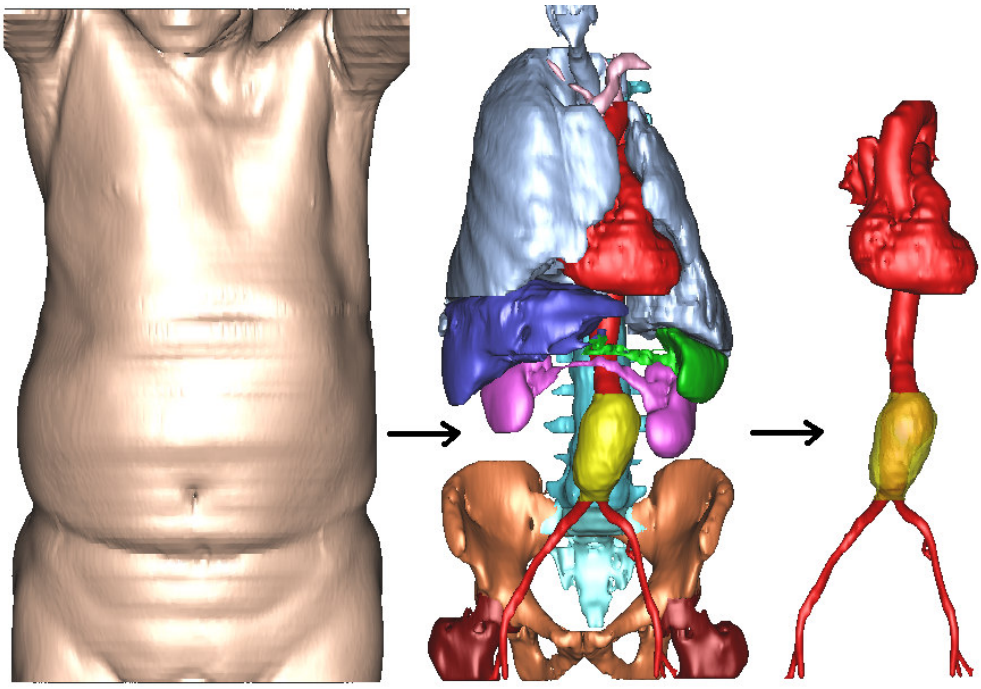

Figure 2: Full 3D reconstruction of CT scan data set. Image shows the use of layers to highlight/remove particular regions of interest depending on desired areas.

3D Reconstructions for Surgical Guidance

CT scan data was obtained from the Midwestern Regional Hospital, Limerick, and St. James's Hospital, Dublin, for 4 patients awaiting EVAR of an AAA. All patients were male with a mean age of 77.5yrs (range 59-87yrs). CT scans were obtained using a Somotom Plus 4 (Siemens AG, D-91052 Erlangen, Germany). The mean pixel size of the CT scans was 0.675mm with all scans taken using a 3mm slice increment. The CT scans were imported into the commercially available software Mimics v12 for reconstruction. For these particular pre-operative reconstructions, only the lumen regions were of clinical importance as this is the region to which the stent-graft is deployed and fixated.

Wall Stress Analysis

The ten 3D reconstructions were imported into the commercial finite element solver ABAQUS v6.7 (Dassault Systemes, SIMULIA, R.I., USA) for stress analysis. In order to simulate *in vivo* wall stress in the AAA wall, realistic boundary conditions were applied to each model. The AAA wall was modelled as a homogenous isotropic hyperelastic material using the finite strain constitutive model proposed by Raghavan and Vorp.[6] These material properties have been utilised in many previous stress

analysis studies. [4,6-8,14,15,20-25] The aorta is also known to be nearly incompressible with a Poisson's ratio of 0.49. The ILT was modelled as a hyperelastic material using the material characterisation derived from 50 ILT specimens from 14 patients performed by Wang et al.[26] Each AAA was constrained in the proximal and distal regions to simulate tethering to the aorta at the renal and iliac bifurcations. The blood pressure within the AAA acts on the luminal contour of the ILT and therefore, pressure was applied to the inner surface of the computational AAA model. A static peak systolic pressure of 120mmHg (16KPa) was used, as employed in most AAA stress analyses. It is known that patient-specific blood pressures may be higher than 120mmHg, but for the purpose of this study a standard value was more appropriate so as to eliminate some of the unknown variables in the analysis. The shear stress induced by blood flow was neglected in this study, although the effects of blood flow have been shown to reduce wall stress in idealised AAA models.[27] Residual stresses that may exist within the aortic wall *in vivo* and tethering forces on the posterior surface caused by the lumbar arteries were also neglected. In addition to these 10 patients, FEA was used to determine the resulting wall stress distributions for the extremely diseased case shown in Figure 3. This particular case experienced a descending thoracic aortic aneurysm (TAA), an abdominal aortic aneurysm (AAA), and also an iliac aortic aneurysm (IAA), and represents a very complex form of aneurismal disease. This model was meshed using shell elements. The intraluminal thrombus (ILT) was omitted from this aspect of the analysis. Mesh independence was performed for all AAA models in order to determine the optimum number of elements, and therefore, the optimum mesh. Mesh independence was performed by increasing the number of elements in the mesh until the difference in peak stress was less than 2% of the previous mesh.[11,14,15,24,28]

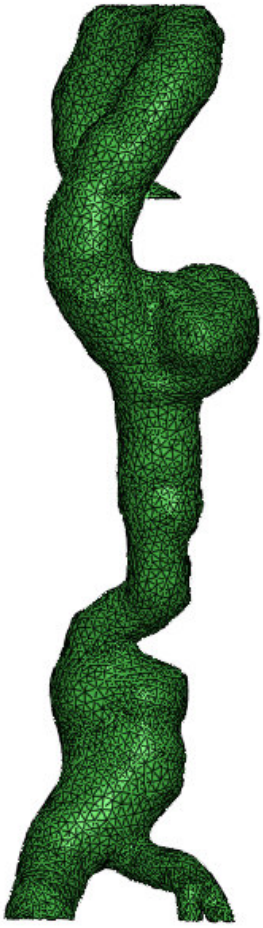

Figure 3: Meshed reconstruction for use in FEA. Case shown is that of an extremely diseased aorta with TAA, AAA and also IAA. Case shown here is from the posterior viewpoint.

FEARI Rupture Assessment

The Finite Element Analysis Rupture Index (FEARI) is defined by Eqn. 2. In this equation, the peak wall stress is computed using the FEM, whereas, the wall strength values are obtained from previous research on experimental testing of AAA wall specimens.[29-31]

$$\text{FEARI} = \frac{\text{FEA Wall Stress}}{\text{Experimental Wall Strength}} \qquad \text{Eqn. 2}$$

This equation is based on the simple engineering definition of material failure, that is, failure will occur when the stress acting on the material exceeds the strength of the material. This index then returns a value ranging from 0 to 1, where 0 indicates a

very low rupture potential, and a value close to 1 indicates a very high rupture potential.

In order to determine strength values for the AAA wall, the previous research of both Raghavan et al.[29,31] and Thubrikar et al.[30] were analysed. These publications are the most detailed reports of experimental uniaxial testing of AAA tissue. Raghavan et al.[29] tensile tested 52 specimens of AAA tissue and found that the average ultimate tensile strength (UTS) of this aneurysmal tissue was 0.942MPa. Thubrikar et al.[30] later segmented AAAs into posterior, anterior and lateral regions and tensile tested 49 tissue specimens. Average regional UTS values were shown to be 0.46MPa, 0.45MPa and 0.62MPa, respectively. Raghavan et al.[31] subsequently furthered their work, and also divided each AAA into regional sections and tested 48 samples. They showed that the UTS of AAA tissue can range from 0.336 – 2.35MPa. They also reported that the regional variations in UTS for the anterior, posterior, left and right regions, were 1.099MPa, 1.272MPa, 1.217MPa and 1.224MPa, respectively.

By combining all the previously published experimental data,[29-31] average regional UTS values for the four main regions of the AAA could be obtained. By subdividing the AAA into a further four sections, eight in total, more regionally accurate strength estimates were obtained, thus allowing FEARI values to be calculated. The method of dividing each AAA into regions is shown in Figure 4, with the resulting UTS values for the varying regions shown in Table 2.

Table 2: Regional UTS values obtained by combining and averaging previous experimental data[29-31]

AAA Region	***UTS (MPa)***
Anterior	0.7744
Posterior	0.8658
Left	0.9221
Right	0.9187
Anterior/Left	0.8482
Anterior/Right	0.8465
Posterior/Left	0.8939
Posterior/Right	0.8922

Once the combined UTS values of AAA tissue were calculated, these values could be coupled with the computed wall stress results from the FEM. By recording the location of peak stress in each AAA model, the region can also be assigned a regional UTS value. FEARI was then computed for each of the ten cases. Statistical analysis was performed on all results using a Pearson's correlation, with $P<0.05$ accepted as significant.

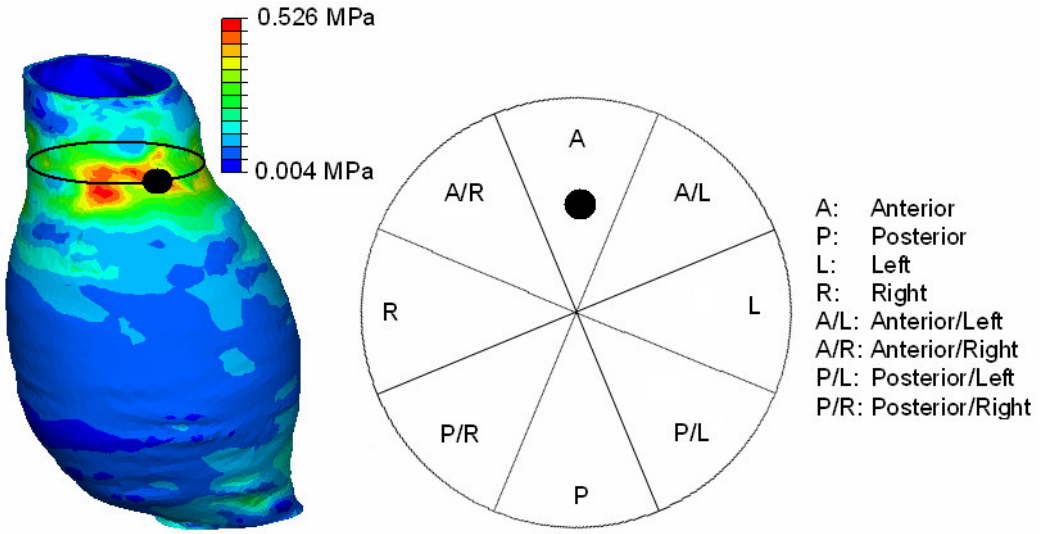

Figure 4: Illustration showing a representative AAA stress distribution for Patient 9 (ellipse passes through region of peak stress, indicated by black circle) and how each AAA model was segmented in order to determine the corresponding UTS value for the particular region of peak stress. In this case, peak stress occurs on the anterior wall of the AAA. AAA model shown in the anterior view.

RESULTS

Wall Stress Results

The finite element analyses using ABAQUS v6.7 produced detailed stress distributions on each of the models under the pressure loading. The von Mises stress is a stress index especially suited for failure analysis, as stress is a tensor quantity with nine components, with the von Mises stress being a combination of these components. By observing the stress distributions, it was noted that the regions of elevated and peak wall stresses occurred at inflection points on the AAA surface, and not at regions of maximum diameter. Inflection points have been previously reported to act as stress raisers on the surface of aneurysms. This observation was also observed by previous

researchers in idealised models, both experimentally[18] and numerically,[13,32] and also in realistic models.[14,15,24] Inflection points are defined as points on the AAA surface at which the local AAA wall shape changes from concave outward to concave inward.[13] The peak wall stresses found in this study ranged from 0.3167 – 1.282MPa, with a mean ± standard deviation of 0.6201 ± 0.2836MPa. The results of the computational stress analysis, along with the maximum diameter and UTS for each case can be seen in Table 3. There was no statistical significance between peak wall stress and any geometrical parameters analysed here. There was however a significant relationship between both FEARI and maximum diameter (*P=0.043*), and FEARI and AAA volume (*P=0.036*).

Table 3: Maximum diameter, FEA computed peak wall stress, location of peak wall stress, and UTS of peak stress region in all ten cases examined. Wall thickness was incorporated in peak wall stress calculations.

Patient	***Max Diameter (cm)***	***Peak Wall Stress (MPa)***	***Location***	***UTS (MPa)***
1	5.1	0.4291	Anterior	0.7744
2	5.8	0.3167	Left	0.9221
3	5.9	0.4346	Anterior/Right	0.8465
4	5.0	0.6641	Anterior/Right	0.8465
5	5.9	0.5866	Anterior/Right	0.8465
6	7.4	0.707	Right	0.9187
7	5.3	0.4	Anterior/Right	0.8465
8	6.2	1.282	Anterior	0.7744
9	6.5	0.5263	Anterior	0.7744
10	9.0	0.855	Posterior	0.8658

The resulting wall stress distributions for the case shown in Figure 3 revealed that the TAA experienced higher stresses than that of both the AAA and IAA. The peak wall stress was 1.336MPa and was located at an inflection point at the proximal region of the TAA, as shown in Figure 5. The failure strength of thoracic aortic aneurysmal tissue has been reported to be approximately 1.19MPa,[33] and since it is known that rupture will occur when local wall stress exceeds local wall strength, these findings provided further support for the clinical intervention.

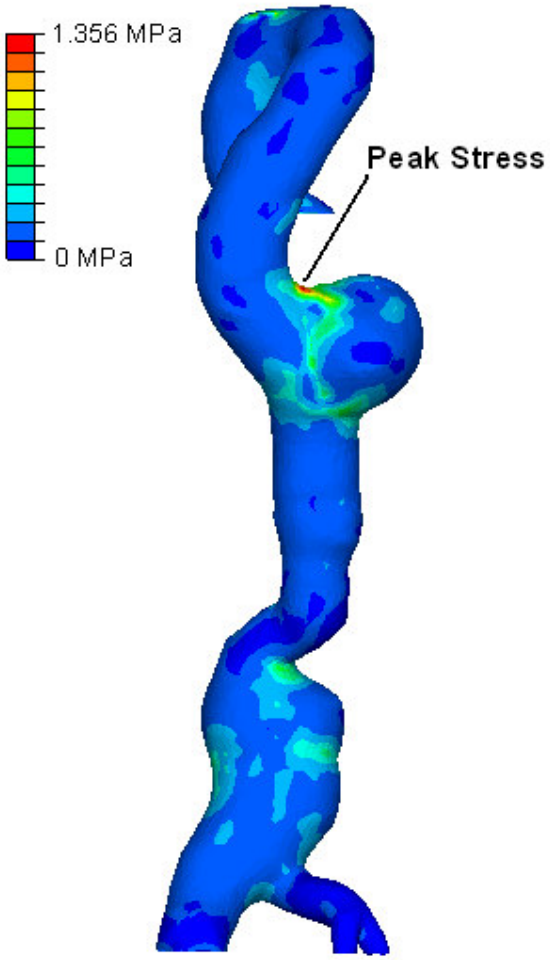

Figure 5: Resulting wall stress distribution for case examined using FEA. Peak stress was located at the proximal inflection point of the TAA. High stress is shown in red in the figure. Lower stresses were observed in both the AAA and the IAA.

FEARI Results

Once all peak wall stresses, locations of peak wall stress, and corresponding regional UTS values were obtained and grouped, FEARI results using Eqn. 2 could be calculated. Table 4 and Figure 6 show the resulting FEARI values with the corresponding maximum diameters of each patient. In this figure, an indication of the possible rupture risk using the FEARI analysis of each patient is shown. An example calculation of this index for Patient 9 can be seen below.

$$\text{FEARI} = \frac{\text{FEA Wall Stress}}{\text{Experimental Wall Strength}} \qquad \text{Eqn. 2}$$

Where, peak FEA wall stress is 0.5263 MPa, and this peak stress occurred in the anterior region of the AAA. Therefore, the UTS of the peak stress region is 0.7744MPa using Table 2. Eqn. 2 now becomes Eqn. 3.

$$\text{FEARI} = \frac{0.5263}{0.7744} = 0.6796 \qquad \text{Eqn. 3}$$

The resulting FEARI for Patient 9 is 0.6796, representing a possible 68% chance of rupture.

Table 4: Resulting FEARI values compared to the corresponding maximum diameters for each AAA studied.

Patient	*Maximum Diameter (cm)*	*FEARI*
1	5.1	0.5541
2	5.8	0.3435
3	5.9	0.5133
4	5.0	0.7845
5	5.9	0.6929
6	7.4	0.7696
7	5.3	0.4725
8	6.2	1.6554
9	6.5	0.6796
10	9.0	0.9876

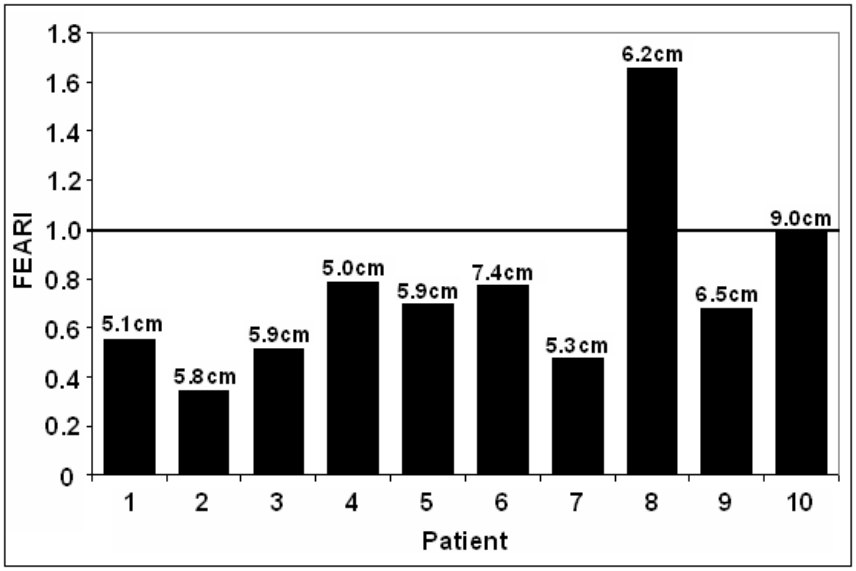

Figure 6: Graph displaying FEARI results for all ten cases. Horizontal line indicates possible AAA rupture based on the FEARI model. Diameters of each case are presented also, indicating how diameter is not related to FEARI.

Surgical Guidance Reconstructions

Four patients awaiting surgical repair were reconstructed into virtual 3D models for examination. Reconstruction times can range from as little as 2 minutes for a basic model where minor details are ignored, to 1 hour where all details are included such as ILT and surface indentations. The critical dimensions when concerned with EVAR stent-grafts are the neck diameter of the stent-graft, the iliac diameter, and also the length of the device. Clinician's can usually determine the neck diameter without difficulty using 2D CT scans, but difficulties can arise when determining length. 3D reconstruction allows the overall length to be easily measured, thus allowing the exact sizing of the medical device. An example of this AAA length measurement can be seen in Figure 7. The measurements are taken from below the lowest renal artery to a point in the iliac arteries where the clinician fells comfortable will maintain an adequate fixation of the device.

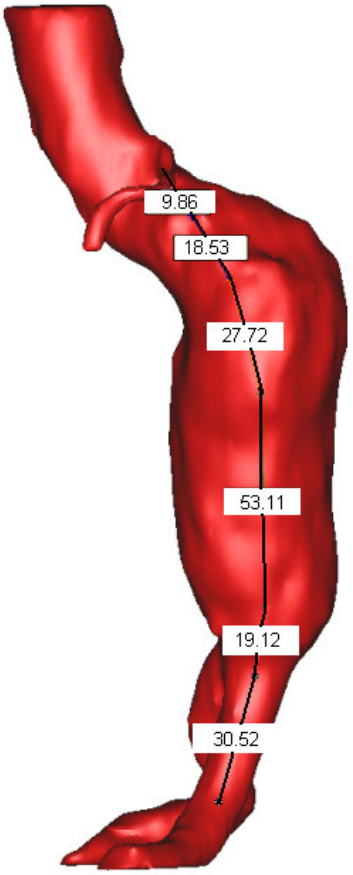

Figure 7: Example reconstruction showing measurements used to size stent-graft. All measurements are in millimeters (mm). Total length of stent-graft was determined to be 159mm.

Concerns arose about one particular patient when CT scans revealed an extremely tortuous proximal neck that may cause difficulties during the surgical procedure. 3D reconstruction highlighted the degree of curvature of the neck and allowed the clinician to decide on the most suitable approach before EVAR. As shown in Figure 8, the proximal neck of the AAA required special attention during the operation. As the upper portion of the stent-graft is embedded into the proximal neck, the tortuous nature of this could complicate placement and fixation of the device.

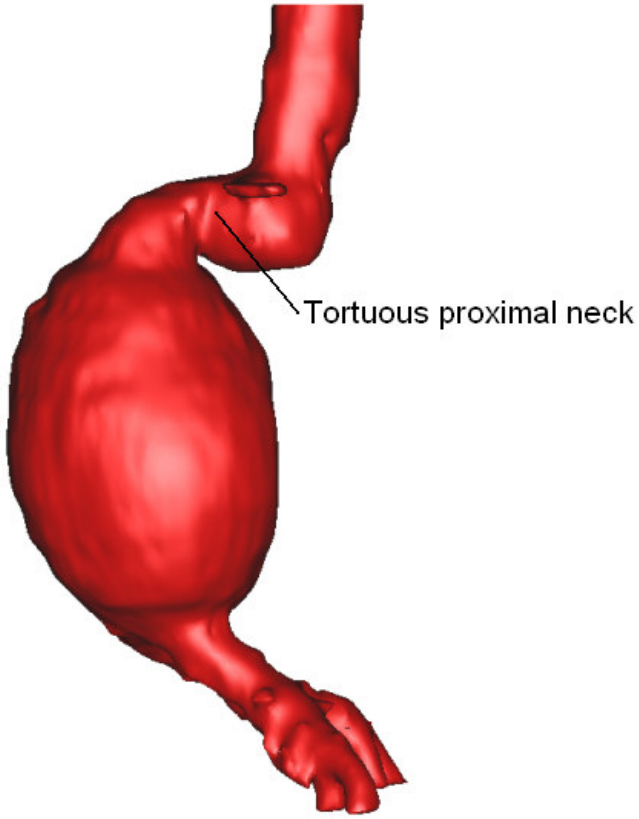

Figure 8: 3D reconstruction revealed extremely tortuous proximal neck which can be identified using 2D CT scans. The 3D reconstruction however, showed exactly the degree of tortuosity, thus allowing the clinician to decide on the most suitable means of approach during EVAR.

The patient-specific reconstruction shown in Figure 9 was a particularly extreme case. In this reconstruction, the full extent of the aneurysmal aorta was revealed. This patient had a descending thoracic abdominal aneurysm (TAA), abdominal aortic aneurysm (AAA) and also an iliac aortic aneurysm (IAA).

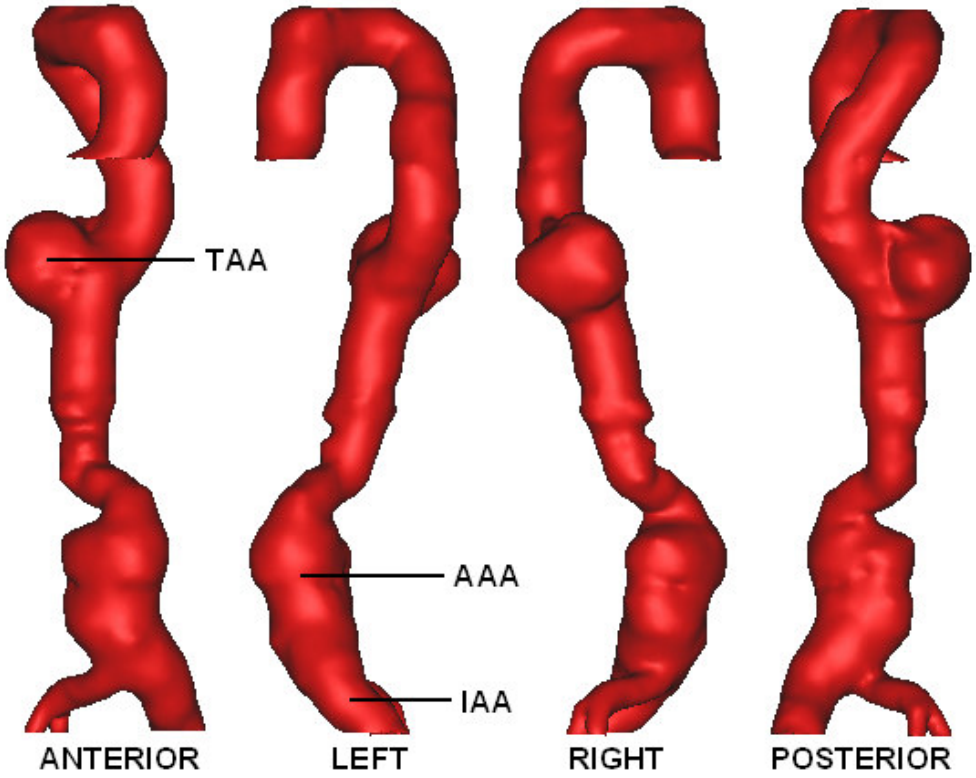

Figure 9: 3D reconstruction showing thoracic aortic aneurysm (TAA), abdominal aortic aneurysm (AAA) and iliac aortic aneurysm (IAA) from various viewpoints.

DISCUSSION

FEARI Rupture Assessment

It is known that AAA rupture occurs when the locally acting wall stress exceeds the locally acting wall strength, and thus the inclusion of wall strength as a rupture parameter may also be useful. The FEARI approach presented here utilises previously published experimental data from tissue specimens[29-31] which were applied to establish FEARI results. The wall stress was computed using the commercial FEA solver, ABAQUS v6.7, from which, peak wall stress values and the location of peak stress could be recorded for each case. Convergence studies were also performed on each model to establish confidence in the finite element mesh size and accuracy of the results.[11,14,15,24,28] Patient-specific wall thickness values were applied to each case using the equation proposed by Li and Kleinstreuer[19] to provide more realistic results. Peak stresses varied throughout the ten cases, and were independent of the maximum diameter of the AAA. There was no statistical significance between peak wall stress and any of the measured parameters (maximum diameter, $P=0.227$; sex, $P=0.404$; AAA volume, $P=0.936$; AAA length, $P=0.501$; ILT volume, $P=0.247$; wall

thickness, *P=0.375*; location of peak stress, *P=0.54*). FEARI results were also statistically compared with the same parameters. Of these comparisons, FEARI was statistically significant with maximum diameter (*P=0.043*) and AAA volume (*P=0.036*), whereas, there was no significance with other parameters (sex, *P=0.961*; AAA length, *P=0.804*; ILT volume, *P=0.881*; wall thickness, *P=0.056*; location of peak stress, *P=0.755*). These results alone suggest that other rupture indicating parameters should be included in the surgical decision-making process. From the ten cases examined, all AAAs experienced peak wall stress at areas where the ILT was regionally thinner, therefore supporting the hypothesis that ILT reduces wall stress by acting like a "mechanical cushion"[11,28,34] for the AAA wall. Another interesting observation relates to Patient 8. In this case, the AAA geometry had a rapid change in diameter from 33.4mm to 61.4mm over 12.5mm. This sudden change in geometry resulted in a large peak stress of 1.282 MPa, which is approximately 60% higher than the similarly sized-diameter AAA of Patient 9.

A FEARI value was determined for each case from Eqn. 2. A FEARI value close to or above 1, suggests that the AAA may be a high rupture-risk AAA, and should be repaired immediately. FEARI values closer to 0, on the other hand, would indicate that the risk of rupture is low, and should be monitored closely through regular ultrasound or CT scanning. All ten cases examined had reached or exceeded the current 5.0cm threshold for surgical repair. At the time of this study, all cases were awaiting or had undergone either traditional open repair or endovascular aneurysm repair (EVAR). The results show that smaller AAAs can have higher peak wall stresses than larger AAAs (see Table 3). Wall stress is closely related to geometrical parameters, with highly stressed areas occurring at regions of inflection on the surface on the AAA. Tortuous and irregularly shaped, or asymmetric, AAAs can experience many regions of inflection, and thus, many regions acting as stress raisers on the surface.

Although FEARI results presented here are preliminary, in that they currently use experimental data from other researchers,[29-31] the approach may be clinically useful. In order to gauge the effect of the UTS on the resulting FEARI, the "worst case scenario" in terms of UTS was examined. Raghavan et al.[31] reported that the UTS of AAA tissue can range from 0.336 – 2.35MPa, and therefore, this minimum strength of

0.336MPa was applied to our FEARI equation. The results can be seen in Figure 10. This resulted in much higher rupture potentials for all ten cases, and suggested that all patients were suitable for immediate repair. Although this minimum UTS value was recorded, only 8 of the 48 specimens tested by Raghavan et al.[31] resulted in UTS values below 0.5MPa, with 0.336MPa being the absolute minimum displayed by any specimen. Therefore, to assume that all AAAs, in all regions experience this low failure stress would appear to be overly conservative.

It is proposed that FEARI could serve as a useful adjunct to diameter-based surgical decision making. Diameter, and ultimately size, of the AAA is an obvious concern for the clinician, and must remain a consideration. The overall geometry of the aneurysm should also play a role. Asymmetry has been shown to affect wall stress in idealised AAA models[13,27,32] and may also affect realistic cases.[14] Other researchers have proposed the Rupture Potential Index (RPI)[35] which uses a statistical modelling technique with the inclusion of factors such as age, gender, family history, smoking status, among others, to deduce patient-specific wall strength.[2] This RPI approach uses a more theoretical method of calculating wall strength, compared to the experimental approach of FEARI, and combining the two approaches may lead to improved predictions. Ultimately, the decision to surgically intervene may include a combination of factors including diameter, asymmetry, RPI and FEARI, along with clinical experience, and may determine the most suitable approach to a particular AAA.

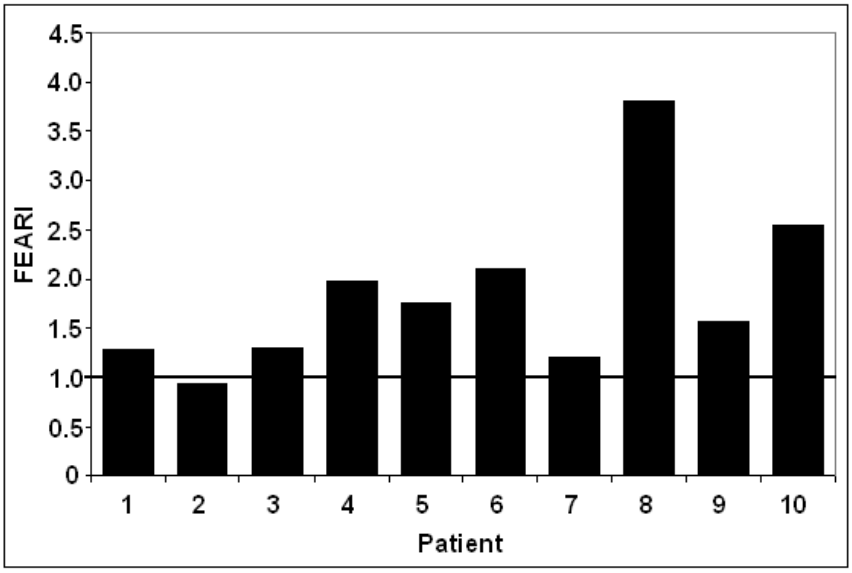

Figure 10: FEARI results for the "worst case scenario" of extremely low failure strengths of the AAA tissue. Horizontal line indicates possible AAA rupture using the FEARI model.

EVAR Surgical Guidance

This aspect of the paper was to highlight the use of 3D reconstruction as a surgical guidance tool for vascular surgeons. Currently, many clinicians use 2D CT scans to determine the correct sizing of stent-grafts and also to visualise the aneurysm prior to surgery. 3D reconstructions provide a useful addition to 2D measurements for stent-graft sizing, and therefore can possibly help improve the outcome of EVAR. This increases surgical confidence in the operation, as the clinician will not encounter any unforeseen geometrical obstacles to the already difficult procedure. Measurements obtained from 2D CT scans are often accurate, in particular when measuring diameter, as the measurement must be taken in a plane perpendicular to the true lumen of the vessel. Many clinicians measure stent-graft length from 2D images as the tortuous nature of the anerysmatic aorta can often be reduced with the introduction of the stiff guide wire. A combination of the methods may provide a better approximation of the exact length, thus allowing more precise stent-graft lengths to be obtained. Measurements from the virtual 3D model however, offer further insight into the morphology of the diseased aorta. The sophisticated measurement tools in Mimics provide accurate dimensions of complex geometries. Iliac bifurcation angles can now be accurately measured in order to determine the correct stent-graft for the particular application. Also, when fenestrated stent-grafts are to be utilised, the distances between the mesenteric arteries and the renal arteries can be accurately obtained.

These exact measurements can be difficult to determine from 2D images. It is also common practice to use a graduated measuring catheter placed over the stiff guide wire prior to deployment of the device, in order to ensure the correct length stent-graft is to be introduced. The case presented in Figure 7 was repaired using the Talent™ stent-graft by Medtronic with no complications 2 years post-operation. Reconstruction times can vary depending on the complexity of the case. Most reconstructions can be performed under 1 hour, which should be adequate as the majority of CT scans are taken a considerable time prior to the actual operation. Therefore, the clinician can often afford to examine a 3D reconstruction without sacrificing the health status of the patient.

The reconstruction shown in Figure 8 revealed a tortuous proximal neck and iliac aneurysm, both of which increase the difficulty of EVAR. Fixation of the distal end of the device in the iliac arteries is hampered by the aneurysmal or tortuous artery, and therefore, the device may dislodge and ultimately fail. Calcified or tortuous iliac arteries may also rupture upon insertion or withdrawal of the introducer. The problems associated with irregular iliac arteries were highlighted in 2003 when Guidant were forced to withdraw the Ancure™ stent-graft from the market.[36] The diameter of the iliac arteries is of obvious importance when sizing stent-grafts, but so too is the tortuosity, as the introducer can place large stresses on the artery wall whilst being navigated through the vessel. Nowadays clinicians are tackling more challenging anatomy with EVAR compared to recent years, and therefore, the ability to view the exact morphology of the iliac arteries has clinical relevance, and may not always be possible with 2D CT scans.

Reconstruction also gives the clinician valuable information about the aneurysm before surgery. This ensures that the clinician does not encounter any unforeseen problems upon surgical repair. This was particularly useful for cases where the aneurysm displays extreme tortuosity and curvature, like the cases presented in Figures 8 and 9. Enabling the clinician to visualise the AAA prior to surgery increases confidence in the procedure as the degree of curvature of the neck or iliac arteries can readily be determined. The case presented in Figure 8 was repaired using the Aorifx™ stent-graft by Lombard due to the tortuous nature of the anatomy. This stent-graft showed no complications 1 year post-operation. This patient later died due

to unrelated causes. Extreme cases, such as that of Figure 9, highlight the advantages of using 3D reconstructions as a surgical tool. From the reconstruction, , precise measurements can be determined using Mimics, such as length, degree of curvature, angles, and exact distances over surfaces, therefore aiding in the choice of a patient-specific stent-graft from the range currently available. Cases such as that presented in Figure 9 may often require tailor-made stent-grafts, and the use of 3D reconstructions aid this task. Tailor-made stent-grafts can be designed using the centrelines generated in Mimics from the reconstructions, and the resulting flow patterns can be identified.[37] Therefore, 3D reconstructions greatly aid in the conception and design of new medical devices. Clinicians will usually opt to have a range of device sizes at hand during the operation so that the correct device can be obtained in the event of unforeseen circumstances. Full examinations using 3D reconstructions can help to alleviate this worry.

3D reconstructions also allow the clinical problem to be examined using various software applications. Diseased aortas can now be modelled using complex mathematical software to determine stresses and strains experienced in the wall, and also the complex flow patterns of the blood through the diseased artery allowing for stent-graft design.[37] The results of the FEA studied here show that the aorta is experiencing a peak stress of 1.356MPa at the proximal inflection point of the TAA, which exceeds the average failure strength of tissue in this area as reported previously.[33] FEA also identifies hotspots on the diseased aorta that may indicate possible rupture sites *in vivo*. The reconstruction of the stent-graft after placement within the TAA can be seen in Figure 11. The device now excludes the region of high stress and thus aids to return the aorta to a lower stress state that is relatively safe from rupture. This reconstruction was generated from post-operative CT scans that help to monitor the diseased aorta, and highlight any additional aneurysm growth from endotension,[38] or further progression of the AAA. Post-operative 3D reconstructions can also aid the clinician to observe the outcome of the EVAR procedure at regular intervals. Stent-graft limbs can often become kinked, twisted or occluded by thrombosis,[16] which can complicate the flow of blood and may require further intervention by the clinician. Although these complications can be identified using 2D CT scans, 3D reconstructions allow exact visualisation of the problem and aid towards a better understanding of the overall situation of the patient. Currently,

there is no institution-wide standard regarding stent-graft sizing, with many clinicians opting for their own methods of measurements, particularly lengths. There is still a degree of learning among the EVAR community when concerned with AAA morphology and stent-graft behaviour. The latest generation of the Medtronic Endurant™ graft appears to shorten more in length on deployment than its predecessor, Talent™, due to design modifications. This consequently affects the recommended measurements and sizing by the manufacturer. Ultimately, better imaging and 3D reconstructions can only add to the quality of the endovascular repair.

Figure 11: Post-operative EVAR illustration showing deployed TAA stent-graft excluding TAA sac. Stent-graft now returns blood flow in the descending aorta to a relatively normal state. Transparency of the aorta in the image allows easy visualisation of the device. Model shown from the posterior viewpoint.

CONCLUSIONS

3D reconstruction of AAAs is a powerful and useful tool. FEARI may be clinically useful due to the simplicity of the approach. Rupture occurs when the AAA tissue cannot withstand the locally acting wall stress exerted, and therefore, tissue strength

must be considered when assessing AAA rupture potential. Peak wall stresses were computed, along with the location, and therefore UTS, of peak wall stress region. FEARI results indicate that surgery may not be necessary for all cases, but rather continued monitoring may suit particular patients. It is proposed to couple FEARI together with diameter and other important factors in AAA assessment to allow the clinician a greater understanding of the severity of an individual AAA before deciding on surgical intervention. 3D reconstruction allows the clinician to obtain measurements useful for the sizing of stent-grafts, and also allows the clinician to visualise the aneurysm prior to surgery. Reconstructions are also necessary for further use with FEA which has been shown to be a good method of determining wall stress in the diseased aorta. FEA provides an additional source of information to the clinician and helps towards a greater understanding of the biomechanical behaviour of the anatomy prior to surgery. This preliminary study of a FEARI suggests that further work into this approach may yield more accurate results, and may provide a useful adjunct to the diameter-based approach in surgical decision-making. 3D reconstruction is quick to perform and could not only help towards standardising the measurement and sizing of stent-grafts, but could also aid surgeons in improving the treatment of AAAs.

ACKNOWLEDGEMENTS

The authors would like to thank (i) the Irish Research Council for Science, Engineering and Technology (IRCSET) Grant RS/2005/340 (ii) Grant #R01-HL-060670 from the US National Heart Lung and Blood Institute (iii) Prof. David A. Vorp from the Centre for Vascular Remodelling and Regeneration, University of Pittsburgh and (iv) Michel S. Makaroun, MD, Department of Surgery, University of Pittsburgh, (v) the Department of Vascular Surgery in the Midwestern Regional Hospital, Ireland, in particular, Mr. Eamon Kavanagh, Mr. Paul Burke and Prof. Pierce Grace.

REFERENCES

1. Sakalihasan N, Limet R, Defawe OD. Abdominal aortic aneurysm. Lancet 2005;365(9470):1577-89.
2. Vande Geest JP, Wang DHJ, Wisniewski SR, Makaroun MS, Vorp DA. Towards a non-invasive method for determination of patient-specific wall strength distribution in abdominal aortic aneurysms. Ann Biomed Eng 2006;34(7):1098-1106.
3. Kleinstreuer C, Li Z. Analysis and computer program for rupture-risk prediction of abdominal aortic aneurysms. Biomed Eng Online 2006;5:19.
4. Leung JH, Wright AR, Cheshire N, Crane J, Thom SA, Hughes AD, Xu Y. Fluid structure interaction of patient specific abdominal aortic aneurysms: a comparison with solid stress models. Biomed Eng Online 2006;5:33.
5. Sayers RD. Aortic aneurysms, inflammatory pathways and nitric oxide. Ann R Coll Surg Engl 2002;84(4):239-246.
6. Raghavan ML, Vorp DA. Toward a biomechanical tool to evaluate rupture potential of abdominal aortic aneurysm: identification of a finite strain constitutive model and evaluation of its applicability. J Vasc Surg 2000;33:475-482.
7. Fillinger MF, Marra SP, Raghavan ML, Kennedy FE. Prediction of rupture risk in abdominal aortic aneurysm during observation: wall stress versus diameter. J Vasc Surg 2003;37:724-732.
8. Fillinger MF, Raghavan ML, Marra SP, Cronenwett JL, Kennedy FE. In vivo analysis of mechanical wall stress and abdominal aortic aneurysm rupture risk. J Vasc Surg 2002;36:589-597.
9. Nicholls SC, Gardner JB, Meissner MH, H Johansen K. Rupture in small abdominal aortic aneurysms. J Vasc Surg 1998:28:884-888.
10. Darling RC, Messina CR, Brewster DC, Ottinger LW. Autopsy study of unoperated abdominal aortic aneurysms. The case for early resection. Circulation 1977;56(II):161-164.
11. Wang DHJ, Makaroun MS, Webster MW, Vorp DA. Effect of intraluminal thrombus on wall stress in patient-specific models of abdominal aortic aneurysm. J Vasc Surg 2002;36:598-604.

12. Raghavan ML, Vorp DA, Federle MP, Makaroun MS, Webster MW. Wall stress distribution on three-dimensionally reconstructed models of human abdominal aortic aneurysm. J Vasc Surg 2000;31:760-769.
13. Vorp DA, Raghavan ML, Webster MW. Mechanical wall stress in abdominal aortic aneurysm: influence of diameter and asymmetry. J Vasc Surg 1998;27(4):632-639.
14. Doyle BJ, Callanan A, Burke PE, Grace PA, Walsh MT, Vorp DA, McGloughlin TM. Vessel asymmetry as an additional tool in the assessment of abdominal aortic aneurysms. J Vasc Surg 2009;49(2):443-454.
15. Doyle BJ, Callanan A, Walsh MT, Grace PA, McGloughlin TM. A finite element analysis rupture index (FEARI) as an additional tool for abdominal aortic aneurysm rupture prediction. Vasc Dis Prev 2009;6:75-82.
16. Corbett TJ, Callanan A, Morris LG, Doyle BJ, Grace PA, Kavanagh EG McGloughlin TM. A review of the in vivo and in vitro biomechanical behaviour and performance of postoperative abdominal aortic aneurysms and implanted stent-grafts. J Endovasc Ther 2008;15:468-464.
17. Doyle BJ, Morris LG, Callanan A, Kelly P, Vorp DA, McGloughlin TM. 3D reconstruction and manufacture of real abdominal aortic aneurysms: from CT scan to silicone model. J Biomech Eng 2008;130:034501-5.
18. Morris L, Delassus P, Callanan A, Walsh M, Wallis F, Grace P, McGloughlin T. 3D numerical simulation of blood flow through models of the human aorta. J Biomech Eng 2005;127:767-775.
19. Li Z, Kleinstreur C. A new wall stress equation for aneurysm-rupture. Ann Biomed Eng 2005;33(2):209-213.
20. Raghavan ML, Vorp DA, Federle MP, Makaroun MS, Webster MW. Wall stress distribution on three-dimensionally reconstructed models of human abdominal aortic aneurysm. J Vasc Surg 2000;31:760-769.
21. Venkatasubramaniam AK, Fagan MJ, Mehta T, Mylankal KJ, Ray B, Kuhan G, et al. A comparative study of aortic wall stress using finite element analysis for ruptured and non-ruptured abdominal aortic aneurysms. Eur J Vasc Endovasc Surg 2004;28:168-176.
22. Papaharilaou Y, Ekaterinaris JA, Manousaki E, Katsamouris AN. A decoupled fluid structure approach for estimating wall stress in abdominal aortic aneurysms. J Biomech 2007;40:367-377.

23. Speelman L, Bohra A, Bosboom EMH, Schurink GWH, van de Vosse FN, Makaroun MS, Vorp DA. Effects of wall calcifications in patient-specific wall stress analyses of abdominal aortic aneurysms. J Biomech Eng 2007;129:1-5.
24. Doyle BJ, Callanan A, McGloughlin TM. A comparison of modelling techniques for computing wall stress in abdominal aortic aneurysms. Biomed Eng Online 2007;6:38.
25. Raghavan ML, Fillinger MF, Marra SP, Naegelein BP, Kennedy FE. Automated methodology for determination of stress distribution in human abdominal aortic aneurysm. J Biomech Eng 2005;127:868-871.
26. Wang DHG, Makaroun MS, Webster MW, Vorp DA. Mechanical properties and microstructure of intraluminal thrombus from abdominal aortic aneurysm. J Biomech Eng 2001;123:536-539**.**
27. Scotti CM, Shkolnik AD, Muluk SC, Finol E. Fluid-structure interaction in abdominal aortic aneurysms: effect of asymmetry and wall thickness. Biomed Eng Online 2005;4:64.
28. Truijers M, Pol JA, SchultzeKool LJ, van Sterkenburg SM, Fillinger MF, Blankensteijn JD. Wall stress analysis in small asymptomatic, symptomatic and ruptured abdominal aortic aneurysms. Eur J Vasc Endovasc Surg 2006;33:401-407.
29. Thubrikar MJ, Labrosse M, Robicsek F, Al-Soudi J, Fowler B. Mechanical properties of abdominal aortic aneurysm wall. J Med Eng Tech 2001;25(4):133-142.
30. Raghavan ML, Webster MW, Vorp DA. Ex vivo biomechanical behaviour of abdominal aortic aneurysm: assessment using a new mathematical model. Ann Biomed Eng 1996;24:573-582.
31. Raghavan ML, Kratzberg J, de Tolosa EMC, Hanaoka MM, Walker P, da Silva ES. Regional distribution of wall thickness and failure properties of human abdominal aortic aneurysm. J Biomech 2006;39(16):3010-6.
32. Callanan A, Morris LG, McGloughlin TM. Numerical and experimental analysis of an idealised abdominal aortic aneurysm. European Society of Biomechanics 2004, S-Hertogenbosch, Netherlands.
33. Vorp DA, Shiro BJ, Ehrlich MP, Ergin MA, Griffith BP. Effect of aneurysm on the tensile strength and biomechanical behaviour of the ascending thoracic aorta. Ann Thorac Surg 2003;75:1210-1214.

34. Vorp DA, Vande Geest J. Biomechanical determinants of abdominal aortic aneurysm rupture. Artherioscler Thromb Vasc Biol 2005;25:1558-1566.
35. Vande Geest JP, Di Martino ES, Bohra A, Makaroun MS, Vorp DA. A biomechanics-based rupture potential index for abdominal aortic aneurysm risk assessment. Ann N Y Acad Sci 2006;1085:11-21.
36. Faries PL, Dayal R, Rhee J, Trocciola S, Kent CK. Stent graft treatment for abdominal aortic aneurysm repair: recent developments in therapy. Diseases of the aorta, pulmonary, and peripheral vessels. Curr Opin Cardiol 2004;19(6):551-557.
37. Molony DS, Callanan A, Morris LG, Doyle BJ, Walsh MT, McGloughlin TM. Geometrical enhancements for abdominal aortic stent grafts. J Endovasc Ther 2008;15:518-529.
38. EVAR Trial Participants. Comparison of endovascular aneurysm repair with open repair in patients with abdominal aortic aneurysm (EVAR trial 1), 30-day operative mortality results: randomised controlled trial. Lancet 2004;364:843-848.